Medicinal Chemistry Research (2024) 33:977–988
https://doi.org/10.1007/s00044-024-03235-x

MEDICINAL CHEMISTRY RESEARCH

ORIGINAL RESEARCH ARTICLE

Synthesis and in vitro biological activity of chalcone derivatives as potential antiparasitic agents

Koketso J. Setshedi[1] · Richard M. Beteck[1] · Kayhan Ilbeigi[2] · Dorien Mabille[2] · Guy Caljon[2] · Lesetja J. Legoabe[1]

Received: 11 March 2024 / Accepted: 3 May 2024 / Published online: 21 May 2024

Abstract

Kinetoplastids are a group of flagellated protozoans including medically important parasites of the genus *Trypanosoma* and *Leishmania*. The corresponding diseases have afflicted humans for centuries. In an effort to combat kinetoplastid infections, a set of 21 chalcones was synthesized and evaluated for their in vitro anti-protozoal efficacy against *Trypanosoma brucei*, *Trypanosoma brucei rhodesiense*, *Trypanosoma cruzi*, and *Leishmania infantum*. To ensure safety, these compounds underwent a selectivity evaluation by assessing toxicity against a human lung fibroblast cell line. Compound **K4** exhibited remarkable and selective trypanocidal activity against *T. b. brucei* with IC_{50} value of 0.31 ± 0.27 µM and *T. b. rhodesiense* with IC_{50} value of 0.96 ± 0.86 µM. Compound **K9** also showed significant trypanocidal activity against *T. b. brucei* (IC_{50}: 0.45 ± 0.14 µM) and *T. b. rhodesiense* (IC_{50}: 0.93 ± 0.51 µM). In both compounds, electron withdrawing groups are appended to the styrenyl moiety.

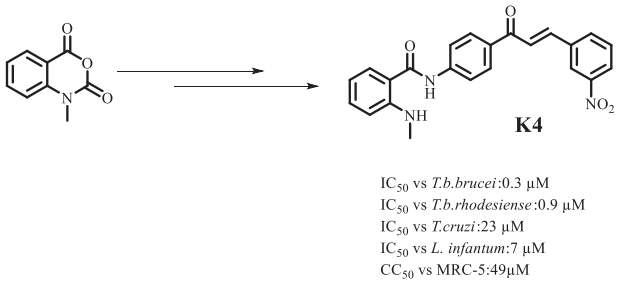

Keywords Anti-protozoal activity · Cytotoxicity · Chalcones · Chagas disease · Sleeping sickness · Visceral leishmaniasis

Introduction

Human African Trypanosomiasis (HAT), sometimes referred to as sleeping sickness is a vector-borne parasitic disease. It is caused by protozoans of the genus *Trypanosoma* and spread by the bite of the blood-sucking tsetse fly (genus *Glossina*) [1]. There are two types of the disease: the slower-progressing form, which is caused by *Trypanosoma brucei gambiense* (*T. b. gambiense*) and is endemic in Western and Central Africa; and the faster-progressing form, which is brought on by *Trypanosoma brucei rhodesiense* (*T. b. rhodesiense*) which is prevalent in Eastern and Southern Africa [2–4]. The parasite causing HAT are endemic in 30 sub-Saharan African countries, wherein 65 million people are at risk of contracting the disease [5].

HAT progresses through two stages: haemolympathic and meningo-encephalitic stages. The haemolympathic stage is characterized by less severe symptoms, including fever and headache. In the meningo-encephalitic stage, the parasites penetrate the blood-brain barrier, causing neuropsychiatric disorders. If left untreated, this stage eventually leads to death [6].

Over the years, a limited number of medications has been authorized for treating sleeping sickness. Pentamidine is

✉ Lesetja J. Legoabe
Lesetja.legoabe@nwu.ac.za

[1] Centre of Excellence for Pharmaceutical Sciences, North-West University, Potchefstroom, South Africa

[2] Laboratory of Microbiology, Parasitology and Hygiene, Infla-Med Centre of Excellence, University of Antwerp, Antwerp 2610, Belgium

registered for treating the first stage of gambiense-HAT, while nifurtimox-eflornithine combination therapy (NECT) is registered for the treatment of second stage gambiense-HAT. NECT is a shorter and safer treatment compared to nifurtimox, or eflornithine monotherapy [7]. A newly registered oral drug, fexinidazole, is recommended for the treatment of both first and second stages of gambiense-HAT, but its use require medical supervision [8]. In rhodesiense-HAT, the first stage is managed using suramin, while the second stage is treated with melarsoprol, an arsenic derivative. Melarsoprol causes fatal reactive encephalopathy in 3–10% of people receiving it [6] Trials for the use of fexinidazole for the treatment of *T. b. rhodesiense*-infected patients are ongoing and a recent report indicates that the drug can be successfully used [9].

Chagas disease (CD), also referred to as American Trypanosomiasis (AT), is a potentially fatal zoonotic disease resulting from infection with the parasite *Trypanosoma cruzi* (*T. cruzi*). This illness is predominantly observed in Central and South America, and the southern regions of the United States [10, 11]. It impacts around 6–8 million individuals globally, leading to roughly 50,000 fatalities annually. Additionally, an estimated 65–100 million people worldwide are at risk of infection [12].

CD is transmitted by triatomine insects, commonly referred to as 'kissing bugs' [13]. The primary mode of transmission occurs when these insects deposit infected fecal material into a wound during/after feeding [13]. Additionally, transmission can take place when hosts consume the infected triatomine or its fecal material [14]. Other routes of transmission include vertical transmission, either through the placenta or maternal milk, direct contact with infected body secretions or blood, transfusions, organ transplantation, contaminated food/drinks and laboratory accidents [12, 15].

Despite more than a century since its identification, CD continues to pose health and economic burden for the majority of Latin American nations [16]. For example, over half a million Disability-Adjusted Life Years (DALY) are lost to CD annually [17–21]. The World Bank and the World Health Organization (WHO) classify CD as the 4th most significant infectious disease, following malaria, tuberculosis, and schistosomiasis [22].

At present, only two drugs, benznidazole and nifurtimox, are available for the treatment of CD [23, 24]. Both benznidazole and nifurtimox can result in diverse adverse side effects which sometimes result in abrupt treatment termination [25]. Benznidazole, favored for its superior safety profile, is typically the primary choice [26]. It is administered orally with daily doses of 5 mg/kg for adults and 7.5 mg/kg for children over 60 days [27].

Visceral leishmaniasis (VL), also known as kala-azar, is a severe sand fly (*Lutzomyia* and *Phlebotomus* sp.)-transmitted illness that poses a significant public health threat. According to the WHO, it is classified as a neglected disease, reaching the second and seventh positions among tropical diseases in terms of mortality and DALY, respectively [28]. Two species of *Leishmania* linked to VL have been identified in West Africa: *Leishmania infatum*, is primarily found in dogs, and causes sporadic human cases and *Leishmania donovani*, which is an anthroponotic [29].

Approximately 13,000 cases of VL were reported in 2020 by the WHO [30, 31]. VL is prevalent in over 70 nations spanning all continents and poses a potential risk to approximately 200 million people. Nonetheless, the distribution of VL is concentrated primarily in seven countries: Brazil, Ethiopia, India, Kenya, Somalia, South Sudan, and Sudan, where over 90% of global VL cases are documented [28, 32–34]. Every year, 500,000 new cases of VL and 50,000 associated deaths are estimated to occur [32].

Chalcones, also known as 1,3-diphenyl-2-propene, are intermediates in the synthesis of several biologically important classes of compounds such as flavones, pyrimidines, pyrazoles, indoles [35]. In several cases, chalcone and its derivatives have been identified from numerous medicinal plants like *Dracaena cinnabari*, *Medicago sativa*, and *Angelica keiskei* [36]. There have been reports of chalcones exhibiting a variety of biological and pharmacological properties such as anti-inflammatory, analgesic, anti-oxidant, anti-bacterial, anti-fungal, anti-viral, anti-tumor, and anti-parasitic activity [37–40]. Figure 1 shows the biological activities of different chalcone derivatives.

Results and discussion

Synthetic chemistry

The compounds of interest were synthesized as outlined in Scheme 1. Amidation reaction between the anhydride (**1**), and aniline (**2**) afforded an amide intermediate (**3**). Intermediate **3** underwent base (NaOH) mediated aldol condensation reaction with appropriate aldehydes to form compound K**1**, K**3**-K1**2**, K**15**-K**23, and K25** in 50–86% yield.

Target compounds were characterized using ^{1}H-NMR, ^{13}C-NMR, HRMS, HPLC and FTIR. The ^{1}H-NMR spectrum displayed a peak at approximately 10.39 ppm, which is characteristics of amide (-CONH-) proton. The singlet peak at ca 2.82 ppm integrating to three protons confirms the presence of N-methyl (NCH_3) group. In the ^{13}C NMR, the amide carbon appears ca 168.33 ppm, and the peak ca 29.37 ppm is assigned to NCH_3. The IR spectra showed

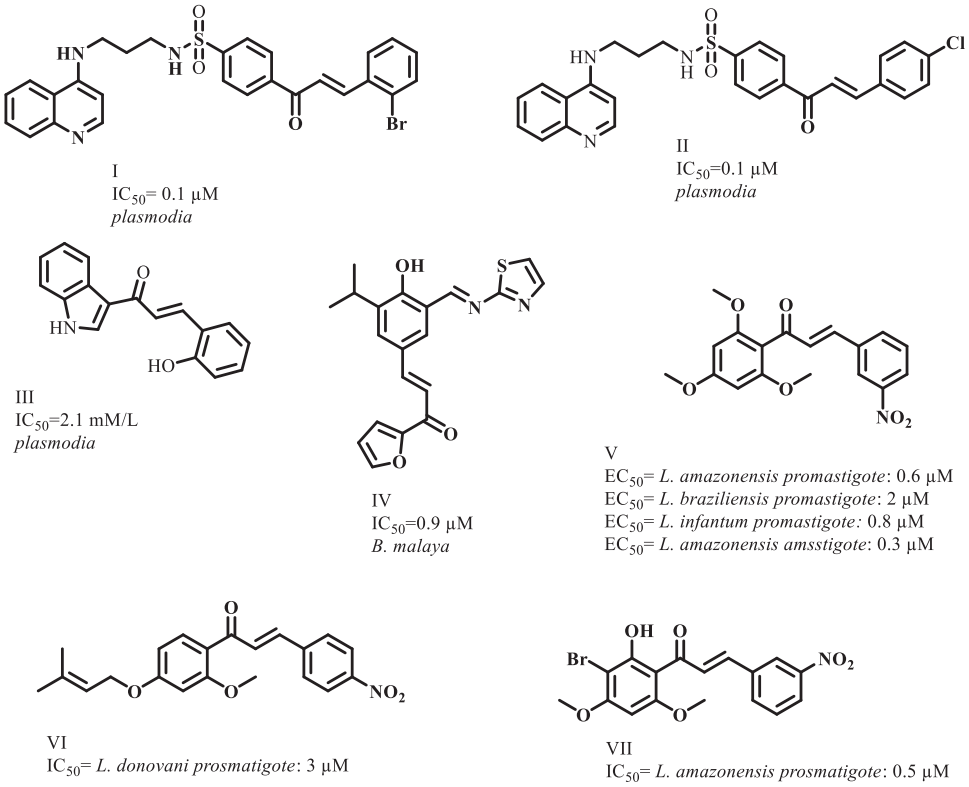

Fig. 1 Biological activities of different chalcone derivatives [36, 43–45]

distinctive absorption bands between 1640–1660 cm^{-1} (C=O), 1570–1605 cm^{-1} (C=C), 675–995 cm^{-1} (C-H bending). The chalcone carbonyl carbon appears ca 188.73 ppm. The high-resolution mass spectrometry (HRMS) established the molecular weight of target compounds, which are consistent with their molecular formulae.

In vitro anti-protozoal activities and cell toxicity

Table 1 below, displays the anti-parasitic activity, cytotoxicity, and selectivity index of the hit compounds. The study examined the anti-kinetoplastid efficacy of the synthesized compounds K**1**, K**3**-K1**2**, K**15**-K**23, and K25** against *T. cruzi*, *T. b. brucei*, *T. b. rhodesiense*, and *L. infantum*. Furthermore, all the synthesized compounds were subjected to counter-screening against the human fetal lung fibroblast (MRC-5) cell line, to explore potential toxicity to human cells. The minimum concentration needed to achieve a 50% (CC_{50}) reduction in cell viability was determined for all compounds.

From the 21 compounds investigated, five anti-trypanosomal hit compounds were identified. Compound **K9** showed modest to potent activity against various parasites deployed in this study. Compound **K4** exhibited sub-micromolar IC_{50} values of 0.31 ± 0.27 μM and 0.96 ± 0.86 μM against *T. b. brucei* and *T. b. rhodesiense*, respectively. Compound **K9** also demonstrated significant activity of 0.45 ± 0.14 μM against *T. b. brucei* and 0.93 ± 0.51 μM against *T. b. rhodesiense*. Compound **K12** demonstrated low micromolar antitrypanosomal activity, with IC_{50} values of 2.49 ± 2.93 μM against *T. b. brucei* and 2.11 ± 1.77 μM against *T. b. rhodesiense*. Compounds **K19** and **K22** demonstrated modest activity in the range of 8–15 μM against both *T. b. rhodesiense* and *T. b. brucei*.

Compounds **K4** and **K9** demonstrated modest and equipotent activity (IC_{50} = 8 μM) against *L. infantum*, while the rest of the compounds exhibited no activity (>64 μM). None of the compounds in this study proved to be active against *T. cruzi*.

Regarding cytotoxicity against MRC-5, compounds in this study were generally not cytotoxic. They exhibited CC_{50} values of >64 μM. Most of the hit compounds exhibit a selectivity index (SI) that exceeds 20 and are thus considered to demonstrate intrinsic and selective anti-*T. brucei* activity. For example, compound **K4** exhibited excellent selectivity, with an SI of 160.

Although the number of active compounds is limited to permit an extensive structure-activity relationship (SARs) analyses, it could generally be observed that the nature and position of substituents on the styrenyl moiety influence antiparasitic activity. *m*-NO_2, and *p*-Cl substituted derivatives showed the best antiparasitic activities, while *ortho*

Scheme 1 Synthesis of target compounds

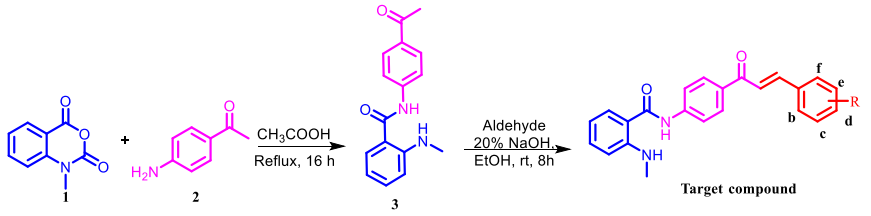

Entry	R	Entry	R	Entry	R	Entry	R
K1		**K7**		**K12**	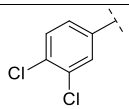	**K19**	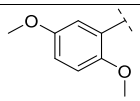
K3	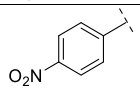	**K8**	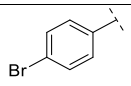	**K15**	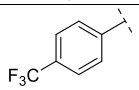	**K20**	
K4	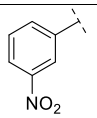	**K9**	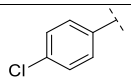	**K16**	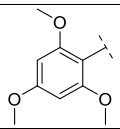	**K21**	
K5	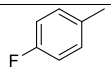	**K10**		**K17**	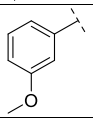	**K22**	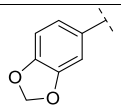
K6	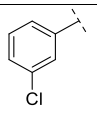	**K11**	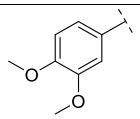	**K18**	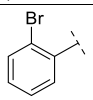	**K23**	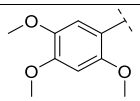
						K25	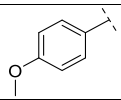

substitution, and derivatives with electron donating substituents were generally not active.

Material and methods

Chemicals and instrumentation

Reagents and solvents were bought from Merck (Pty) Ltd and were utilized as provided. Reactions were monitored through thin layer chromatography (TLC), which used Merck $60F_{254}$ silica gel plates supported on 0.20 mm thick aluminum sheets. Developed plates were visualized with ultraviolet (UV) light at wavelengths of 254 nm and 366 nm or stained in iodine chamber. A Bruker Biospin 600 MHz spectrometer was used to record the ^{1}H and ^{13}C NMR spectra. Chemical shifts are reported relative to residual solvent peaks (DMSO d_6: 2.5 ppm for ^{1}H and 39.5 ppm for ^{13}C). The spectra were processed using MestReNova software. Chemical shifts were quantified in parts per million (ppm), whereas *J*-coupling constants were recorded in hertz (Hz). Signal multiplicities are expressed as follows: s for a singlet, d for a doublet, dd for the doublet of doublet, ddd for the doublet of the doublet of the doublets, t for a triplet and m for multiplet. High-resolution mass spectra (HRMS) were recorded on Bruker micrOTOF-Q II mass spectrometer using atmospheric pressure chemical ionization (APCI) technique in positive ion mode. The melting points (m. pt.) of the target compounds were ascertained using a Büchi® melting point equipment (Model B-545, AC/DC input 230 V AC). For the Fourier-transform infrared spectroscopy (FTIR), a Bruker ALPHA FTIR spectrometer equipped with a Diamond Crystal ATR (Attenuated Total Internal Reflectance) accessory was employed. High- performance liquid chromatography (HPLC) using an Agilent 1200 series HPLC system equipped with a quaternary pump and an Agilent 1200 series diode array detector was used to ascertain the purity of the compound. A Venusil XBP C18 column (4.60 × 150 mm, 5 µm) was used for separation, and the mobile phase consisted of 10% methanol and 90% MilliQ water at a flow rate of 1 mL/min. The compounds were prepared in HPLC grade acetonitrile (ACN), and 10 µL of the sample was injected. The samples were examined at 280 nm and 400 nm wavelengths with a flow rate adjusted to 1 mL/min.

Table 1 This table displays the anti-parasitic activity, cytotoxicity, and Selectivity Index of compounds

Compound Code	Anti-parasitic activity Mean $IC_{50} \pm SD$ (μM)				Cytotoxicity Mean $IC_{50} \pm SD$ (μM)	Selectivity (SI)	Index
	T. cruz	*L. inf*	*T. b. bruc*	*T. b. rhod*	MRC-5	MRC-5 /*T. bruc*	MRC-5 /*T. rhod*
K1	>64	>64	>64	>64	>64	>1	>1
K3	>64	>64	>64	>64	>64	>1	>1
K4	23.62 ± 16.02	7.57 ± 0.62	0.31 ± 0.27	0.96 ± 0.86	49.58 ± 5.73	160	52
K5	>64	>64	>64	>64	>64	>1	>1
K6	>64	>64	>64	>64	>64	>1	>1
K7	>64	>64	>64	>64	>64	>1	>1
K8	>64	>64	>64	>64	>64	>1	>1
K9	19.72 ± 17.37	8.34 ± 4.57	0.45 ± 0.14	0.93 ± 0.51	25.16 ± 4.64	56	27
K10	>64	>64	>64	>64	>64	>1	>1
K11	>64	>64	>64	>64	>64	>1	>1
K12	34.83 ± 0.98	36.42 ± 39.01	2.49 ± 2.93	2.11 ± 1.77	54.26 ± 9.75	>22	>26
K15	>64	>64	>64	>64	>64	>1	>1
K16	>64	>64	>64	>64	>64	>1	>1
K17	>64	>64	>64	>64	>64	>1	>1
K18	>64	>64	>64	>64	>64	>1	>1
K19	45.25	28.51	8.62	8.11	35.01	4.1	4.3
K20	>64	>64	>64	>64	>64	>1	>1
K21	>64	>64	>64	>64	>64	>1	>1
K22	>64	43.55	13.93	15.0	>64	>4.6	>4.3
K23	>64	>64	>64	>64	>64	>1	>1
K25	>64	>64	>64	>64	>64	>1	>1
Benznidazole	**1.35**		–	–	–	–	
Suramine	–	–	**0.04**	**0.05**	–	–	
Miltefosine	–	**7.13**	–	–	–	–	
Tamoxifen	–	–	–	–	**10.79**	–	

Experiments with the most active hits were conducted in independent duplicates, and the data is presented as the mean values (± standard deviation)

T. cruz Trypanosoma cruzi, *L. inf Leishmania infantum*, *T. b. bruc Trypanosoma brucei brucei*, *T. b. rhod Trypanosoma brucei rhodesiense*, *SI* Selectivity Index

Bold values indicate the activity of the reference compounds against the respective parasitic organisms

Synthesis procedure for target compounds

Amide formations

General procedure for synthetic route for N-(4-acetylphenyl)-2-(methylamino)benzamide A round-bottomed flask was charged with *p*-aminoacetophenone (1 g, 5.64 mmol), 1.5 equiv of *N*-methylisatoic anhydride (1.14 g, 8.47 mmol) and 10 mL of glacial acetic acid. The mixture was heated at 100 °C overnight. After the reaction was completed, the content was poured into water. The resulting precipitate was then filtered, dried to give intermediate N-(4-acetylphenyl)-2-(methylamino)benzamide, which was used in the next step without further purification.

Aldol reaction

A mixture of N-(4-acetylphenyl)-2-(methylamino)benzamide, 1.5 equiv of benzaldehyde, aqueous solution of sodium hydroxide (NaOH; 20%, 10 mL), and 30 mL of ethanol was stirred at room temperature for 15 h. The reaction progress was monitored by TLC. After the completion of the reaction, the mixture was poured over crushed ice, acidified with diluted HCl and the precipitated chalcone

was filtered and dried. The crude compound was purified through recrystallization from 95% ethanol to obtain the desired product of 50.16–80.21% yield.

Compounds characterization

(E)-N-(4-(3-(3-fluorophenyl)acryloyl)phenyl)-2-(methylamino)benzamide (K1)

Brown powder, yield of 50.2% and m. pt. 151.0 °C. ^{1}H NMR (600 MHz, DMSO-d_6) δ 10.38 (s, 1H), 8.20 (d, $J = 8.2$ Hz, 2H), 8.03 (d, $J = 15.6$ Hz, 1H), 7.95 (d, $J = 8.3$ Hz, 2H), 7.85 (d, $J = 9.9$ Hz, 1H), 7.73 (s, 1H), 7.72–7.68 (m, 2H), 7.53–7.47 (m, 1H), 7.38 (t, $J = 7.1$ Hz, 1H), 7.28 (t, $J = 8.1$ Hz, 2H), 6.71 (d, $J = 8.2$ Hz, 1H), 6.66 (t, $J = 7.1$ Hz, 1H), 2.82 (s, 3H). ^{13}C NMR (151 MHz, DMSO-d_6) δ 187.43, 168.33, 161.67, 150.21, 143.97, 141.77, 137.34, 133.15, 132.15, 130.80, 130.74, 129.68, 129.07, 125.44, 123.48, 119.60, 116.98, 115.07, 114.03, 110.74, 29.37. IR (ATR) V_{max} cm^{-1}: 3319 (N-H stretching), 1681 (C=O stretching), 1649 (C=C stretching), 1218 (C-F stretching) and 736 (C-H bending). The HRMS (APCI) *m/z* $[M + H]^+$ calculated for $C_{23}H_{20}FN_2O_2$ 375.1503; found 375.1506. Purity (HPLC): 97%. R_t: 2.2 min.

(E)-2-(methylamino)-N-(4-(3-(4-nitrophenyl)acryloyl)phenyl) benzamide (K3)

Mustard powder, yield of 53.47% and m. pt. 189.2 °C. ^{1}H NMR (600 MHz, DMSO-d_6) δ 10.40 (s, 1H), 8.29 (d, $J = 7.8$ Hz, 2H), 8.21 (d, $J = 8.1$ Hz, 2H), 8.17 (d, $J = 7.8$ Hz, 3H), 8.14 (s, 1H), 7.96 (d, $J = 8.1$ Hz, 2H), 7.81 (d, $J = 15.6$ Hz, 1H), 7.73 (d, $J = 7.4$ Hz, 1H), 7.38 (t, $J = 7.2$ Hz, 1H), 6.71 (d, $J = 8.1$ Hz, 1H), 6.66 (t, $J = 7.1$ Hz, 1H), 2.82 (s, 3H). ^{13}C NMR (151 MHz, DMSO-d_6) δ 187.31, 168.33, 150.20, 147.97, 144.16, 141.29, 140.41, 133.17, 131.92, 129.79, 129.73, 129.08, 126.09, 123.85, 119.61, 115.04, 114.05, 110.76, 29.38. IR (ATR) V_{max} cm^{-1}: 3378 (N-H stretching), 1653 (C=O stretching), 1594 (C=C stretching), 1516 (N-O stretching) and 732 (C-H bending). The HRMS (APCI) *m/z* $[M + H]^+$ calculated for $C_{23}H_{20}N_3O_4$ 402.1448; found 402.1440. Purity (HPLC): 95%. R_t: 2.2 min.

(E)-2-(methylamino)-N-(4-(3-(3-nitrophenyl)acryloyl)phenyl) benzamide (K4)

Mustard powder, yield of 80.21% and m. pt. 102.1–102.2 °C. ^{1}H NMR (600 MHz, DMSO-d_6) δ 10.39 (s, 1H), 8.78 (s, 1H), 8.33 (d, $J = 7.1$ Hz, 1H), 8.26 (d, $J = 7.8$ Hz, 1H), 8.23 (d, $J = 8.1$ Hz, 2H), 8.18 (d, $J = 15.7$ Hz, 1H), 7.96 (d, $J = 8.1$ Hz, 2H), 7.84 (d, $J = 15.6$ Hz, 1H), 7.76 (d, $J = 7.7$ Hz, 1H), 7.73 (d, $J = 8.4$ Hz, 1H), 7.38 (t, $J = 7.1$ Hz, 1H), 7.34 (s, 1H), 6.73–6.64 (m, 2H), 3.31 (s, 3H).^{13} C NMR (151 MHz, DMSO-d_6) δ 187.36, 168.34, 150.23, 148.41, 144.09, 140.73, 136.70, 134.98, 133.16, 132.01, 130.27, 129.80, 129.08, 124.79, 124.47, 122.86, 119.58, 115.04, 114.01, 110.72, 29.36. IR (ATR) V_{max} cm^{-1}: 3347 (N-H stretching), 1649 (C=O stretching), 1609 (C=C stretching), 1509 (N-O stretching) and 740 (C-H bending). The HRMS (APCI) *m/z* $[M + H]^+$ calculated for $C_{23}H_{20}N_3O_4$ 402.1448; found 402.1443. Purity (HPLC): 97%. R_t: 2.2 min.

(E)-N-(4-(3-(4-fluorophenyl)acryloyl)phenyl)-2-(methylamino)benzamide (K5)

Brown powder, yield of 86% and m. pt. 171.7–174.1 °C. ^{1}H NMR (600 MHz, DMSO-d_6) δ 10.38 (s, 1H), 8.18–8.08 (m, 2H), 7.97 (d, $J = 4.4$ Hz, 2H), 7.94 (t, $J = 10.7$ Hz, 3H), 7.78–7.68 (m, 2H), 7.38 (d, $J = 5.6$ Hz, 1H), 7.30 (d, $J = 4.4$ Hz, 3H), 6.73–6.68 (m, 1H), 6.66 (d, $J = 5.0$ Hz, 1H), 2.81 (s, 3H). ^{13}C NMR (151 MHz, DMSO-d_6) δ 187.46, 168.32, 164.12, 150.22, 143.83, 142.03, 133.14, 132.31, 131.45, 131.05, 129.57, 129.06, 121.93, 119.60, 115.92, 115.08, 114.02, 110.72, 29.36. IR (ATR) V_{max} cm^{-1}: 3356 (N-H stretching), 1648 (C=O stretching), 1608 (C=C stretching), 1334 (C-F stretching) and 740 (C-H bending). The HRMS (APCI) m/z $[M + H]^+$ calculated for $C_{23}H_{20}FN_2O_2$ 375.1503; found 375.1496. Purity (HPLC): 95%. R_t: 2.2 min.

(E)-N-(4-(3-(3-chlorophenyl)acryloyl)phenyl)-2-(methylamino)benzamide (K6)

Dark brown powder, yield of 50.80% and m. pt. 157.5 °C. ^{1}H NMR (600 MHz, DMSO-d_6) δ 10.39 (s, 1H), 8.21 (d, $J = 8.0$ Hz, 2H), 8.07 (d, $J = 11.0$ Hz, 2H), 8.04 (s, 1H), 7.95 (d, $J = 8.2$ Hz, 2H), 7.82 (d, $J = 5.3$ Hz, 1H), 7.71 (t, $J = 11.1$ Hz, 2H), 7.53–7.46 (m, 2H), 7.38 (t, $J = 7.0$ Hz, 1H), 6.76–6.63 (m, 2H), 2.82 (s, 3H). ^{13}C NMR (151 MHz, DMSO-d_6) δ 187.39, 168.33, 150.21, 143.98, 141.54, 137.05, 133.76, 133.15, 132.14, 130.61, 129.94, 129.71, 129.07, 127.81, 127.78, 123.55, 119.59, 115.08, 114.04, 110.74, 29.37. IR (ATR) V_{max} cm^{-1}: 3355 (N-H stretching), 1651 (C=O stretching), 1592 (C=C stretching), 737 (C-Cl stretching) and 737 (C-H bending). The HRMS (APCI) *m/z* $[M + H]^+$ calculated for $C_{23}H_{20}ClN_2O_2$ 391.1208; found 391.1195. Purity (HPLC): 95%. R_t: 2.2 min.

(E)-2-(methylamino)-N-(4-(3-(o-tolyl)acryloyl)phenyl) benzamide (K7)

Lime green powder, yield of 66.64% and m. pt. 185.9 °C. ^{1}H NMR (600 MHz, DMSO-d_6) δ 10.46 (s, 1H), 8.17 (d,

$J = 8.2$ Hz, 2H), 7.99 (d, $J = 6.1$ Hz, 2H), 7.98–7.94 (m, 3H), 7.83 (d, $J = 15.5$ Hz, 1H), 7.76 (d, $J = 7.5$ Hz, 1H), 7.41 (t, $J = 7.4$ Hz, 1H), 7.37–7.32 (m, 1H), 7.29 (s, 2H), 6.80 (d, $J = 8.1$ Hz, 1H), 6.74 (t, $J = 7.0$ Hz, 1H), 2.84 (s, 3H), 2.45 (s, 3H).^{13}C NMR (151 MHz, DMSO-d$_6$) δ 187.62, 168.07, 149.03, 143.77, 140.39, 137.85, 133.39, 133.12, 132.41, 130.73, 130.20, 129.58, 129.16, 126.81, 126.32, 122.94, 119.69, 116.25, 115.30, 111.87, 30.04, 19.31. IR (ATR) V_{max} cm^{-1}: 3306 (N-H stretching), 1657 (C=O stretching), 1597 (C=C stretching), 741 (C-H bending). The HRMS (APCI) *m/z* $[M + H]^+$ calculated for $C_{24}H_{23}N_2O_2$ 371.1754; found 371.1736. Purity (HPLC): 99%. R_t: 2.2 min.

(E)-N-(4-(3-(4-bromophenyl)acryloyl)phenyl)-2-(methylamino)benzamide (K8)

Light brown powder, yield of 80.13% and m. pt. 190.9 °C. ^{1}H NMR (600 MHz, DMSO-d$_6$) δ 10.47 (s, 1H), 8.18 (d, $J = 8.2$ Hz, 2H), 8.01 (s, 1H), 7.98 (s, 1H), 7.95 (d, $J = 8.2$ Hz, 2H), 7.86 (d, $J = 7.9$ Hz, 2H), 7.76 (d, $J = 7.4$ Hz, 1H), 7.71 (s, 1H), 7.69–7.65 (m, 2H), 7.41 (t, $J = 7.3$ Hz, 1H), 6.81 (d, $J = 8.0$ Hz, 1H), 6.75 (t, $J = 6.9$ Hz, 1H), 2.84 (s, 3H). ^{13}C NMR (151 MHz, DMSO-d$_6$) δ 187.47, 168.07, 148.99, 143.87, 141.92, 134.10, 133.15, 132.29, 131.83, 130.69, 129.64, 129.18, 123.77, 122.84, 119.68, 116.27, 115.40, 111.96, 30.10. IR (ATR) V_{max} cm^{-1}: 3380 (N-H stretching), 1656 (C=O stretching), 1605 (C=C stretching), 673 (C-Br stretching) and 749 (C-H bending). The HRMS (APCI) *m/z* $[M + H]^+$ calculated for $C_{23}H_{20}BrN_2O_2$ 435.0703, found 435.0705. Purity (HPLC): 95%. R_t: 2.2 min.

(E)-N-(4-(3-(4-chlorophenyl)acryloyl)phenyl)-2-(methylamino)benzamide (K9)

Mustard powder, yield of 54.92% and m. pt. 167.1 °C. ^{1}H NMR (600 MHz, DMSO-*d*$_6$) δ 10.38 (s, 1H), 8.18 (d, $J = 8.4$ Hz, 2H), 8.00 (s, 1H), 7.96 (d, $J = 10.9$ Hz, 2H), 7.93 (d, $J = 8.2$ Hz, 3H), 7.74–7.70 (m, 2H), 7.53 (d, $J = 8.1$ Hz, 2H), 7.38 (t, $J = 7.7$ Hz, 1H), 6.71 (d, $J = 8.4$ Hz, 1H), 6.66 (t, $J = 7.4$ Hz, 1H), 2.82 (s, 3H). ^{13}C NMR (151 MHz, DMSO-d$_6$) δ 187.43, 168.33, 150.22, 143.91, 141.78, 134.89, 133.76, 133.15, 132.22, 130.44, 129.62, 129.07, 128.88, 122.78, 119.60, 115.07, 114.02, 110.73, 29.36. IR (ATR) V_{max} cm^{-1}: 3321 (N-H stretching), 1652 (C=O stretching), 1590 (C=C stretching), 744 (C-Cl stretching) and 744 (C-H bending). The HRMS (APCI) *m/z* $[M + H]^+$ calculated for $C_{23}H_{20}ClN_2O_2$ 391.1208; found 391.1214. Purity (HPLC): 98%. R_t: 2.2 min.

(E)-N-(4-(3-(2-chlorophenyl)acryloyl)phenyl)-2-(methylamino)benzamide (K10)

Lime green powder, yield of 68.65% and m. pt. 175.2 °C. ^{1}H NMR (600 MHz, DMSO-*d*$_6$) δ 10.50 (s, 1H), 8.22 (d, $J = 7.4$ Hz, 1H), 8.19 (d, $J = 7.9$ Hz, 2H), 8.02 (d, $J = 6.1$ Hz, 2H), 7.97 (t, $J = 9.4$ Hz, 2H), 7.77 (d, $J = 7.8$ Hz, 1H), 7.57 (d, $J = 7.5$ Hz, 1H), 7.47 (dd, $J = 9.4$, 4.3 Hz, 2H), 7.42 (t, $J = 7.7$ Hz, 2H), 6.82 (d, $J = 8.3$ Hz, 1H), 6.76 (t, $J = 7.3$ Hz, 1H), 2.84 (s, 3H).^{13}C NMR (151 MHz, DMSO-d$_6$) δ 187.38, 168.04, 148.79, 144.01, 137.90, 134.25, 133.15, 132.40, 132.11, 131.83, 129.98, 129.74, 129.20, 128.54, 127.65, 124.81, 119.71, 116.47, 115.62, 112.15, 30.21. IR (ATR) V_{max} cm^{-1}: 3314 (N-H stretching), 1658 (C=O stretching), 1602 (C=C stretching) 758 (C-Cl stretching) and 768 (C-H bending). The HRMS (APCI) *m/z* $[M + H]^+$ calculated for $C_{23}H_{20}ClN_2O_2$ 391.1208; found 391.1194. Purity (HPLC): 99%. R_t: 2.2 min.

(E)-N-(4-(3-(3,4-dimethoxyphenyl)acryloyl)phenyl)-2-(methylamino)benzamide (K11)

Brown powder, yield of 51.54% and m. pt. 188.7 °C ^{1}H NMR (600 MHz, DMSO-*d*$_6$) δ 10.47 (s, 1H), 8.18 (d, $J = 7.4$ Hz, 2H), 7.95 (d, $J = 7.3$ Hz, 2H), 7.86 – 7.82 (m, 1H), 7.77 (d, $J = 7.8$ Hz, 1H), 7.69 (d, $J = 15.4$ Hz, 1H), 7.54 (s, 1H), 7.43 (d, $J = 7.6$ Hz, 1H), 7.39 (s, 1H), 7.38 (s, 1H), 7.03 (d, $J = 8.2$ Hz, 1H), 6.83 (d, $J = 8.2$ Hz, 1H), 6.77 (t, $J = 7.1$ Hz, 1H), 3.87 (s, 3H), 3.82 (s, 3H), 2.84 (s, 3H).^{13}C NMR (151 MHz, DMSO-d$_6$) δ 187.48, 168.01, 151.20, 149.04, 148.76, 143.84, 143.56, 133.10, 132.73, 129.46, 129.19, 127.63, 123.79, 119.66, 119.57, 116.59, 115.65, 112.17, 111.61, 110.83, 55.78, 55.61, 30.22. IR (ATR) V_{max} cm^{-1}: 3357 (N-H stretching), 1652 (C=O stretching), 1594 (C=C stretching), 1256 (C-C stretching), and 730 (C-H bending). The HRMS (APCI) *m/z* $[M + H]^+$ calculated for $C_{25}H_{25}N_2O_4$ 417.1778; found 417.1778. Purity (HPLC): 96%. R_t: 2.2 min.

(E)-N-(4-(3-(3,4-dichlorophenyl)acryloyl)phenyl)-2-(methylamino)benzamide (K12)

Mustard powder, yield of 71.92% and m. pt. 195 °C. ^{1}H NMR (600 MHz, DMSO-*d*$_6$) δ 10.39 (s, 1H), 8.28 (s, 1H), 8.21 (d, $J = 8.5$ Hz, 2H), 8.07 (d, $J = 15.6$ Hz, 1H), 7.95 (d, $J = 8.6$ Hz, 2H), 7.87 (d, $J = 8.0$ Hz, 1H), 7.74–7.70 (m, 2H), 7.68 (s, 1H), 7.39 (d, $J = 7.2$ Hz, 1H), 7.37 (s, 1H), 6.71 (d, $J = 8.3$ Hz, 1H), 6.66 (t, $J = 7.3$ Hz, 1H), 2.82 (s, 3H). ^{13}C NMR (151 MHz, DMSO-d$_6$) δ 187.28, 168.33, 150.23, 144.04, 140.44, 135.69, 133.16, 132.51, 132.06, 131.77, 130.91, 130.02, 129.73, 129.07, 129.03, 124.08, 119.58, 115.05, 114.02, 110.73, 29.36. IR (ATR) V_{max} cm

$^{-1}$: 3355 (N-H stretching), 1647 (C=O stretching), 1593 (C=C stretching), 834 (C-Cl stretching) and 741 (C-H bending). The HRMS (APCI) *m/z* $[M + H]^+$ calculated for $C_{23}H_{19}Cl_2N_2O_2$ 425.0801; found 425.0801. Purity (HPLC): 95%. R_t: 2.2 min.

E)-2-(methylamino)-N-(4-(3-(4-(trifluoromethyl)phenyl) acryloyl)phenyl)benzamide (K15)

Yellow powder, yield of 63.22% and m. pt. 202.1 °C. ^{1}H NMR (600 MHz, DMSO) δ 10.42 (s, 1H), 8.22 (s, 1H), 8.20 (s, 1H), 8.12 (d, $J = 7.8$ Hz, 2H), 8.10 (s, 1H), 7.96 (d, $J = 8.7$ Hz, 2H), 7.84 – 7.79 (m, 2H), 7.77 (s, 1H), 7.73–7.71 (m, 1H), 7.40–7.32 (m, 2H), 6.70 (t, $J = 7.2$ Hz, 1H), 6.66 (t, $J = 7.5$ Hz, 1H), 2.81 (d, $J = 4.7$ Hz, 3H). ^{13}C NMR (151 MHz, DMSO-d_6) δ 187.46, 168.42, 150.28, 144.18, 141.34, 138.86, 133.24, 132.05, 129.82, 129.39, 129.16, 125.71, 125.69, 124.73, 119.67, 119.53, 115.08, 114.07, 110.77, 29.41. IR (ATR) V_{max} cm^{-1}: 3364 (N-H stretching), 1653 (C=O stretching), 1592 (C=C stretching), 1319 (C-F stretching) and 743 (C-H bending). The HRMS (APCI) *m/z* $[M + H]^+$ calculated for $C_{24}H_{20}F_3N_2O_2$ 425.1456; found 425.1456. Purity (HPLC): 95%. R_t: 2.2 min.

(E)-2-(methylamino)-N-(4-(3-(2,4,6-trimethoxyphenyl) acryloyl)phenyl)benzamide (K16)

Maroon powder, yield of 54.08% and m. pt. 132.8 °C. ^{1}H NMR (600 MHz, DMSO-d_6) δ 10.36 (s, 1H), 8.08 (t, $J = 12.9$ Hz, 1H), 7.99 (d, $J = 7.6$ Hz, 2H), 7.94–7.88 (m, 3H), 7.71 (d, $J = 7.2$ Hz, 1H), 7.38 (t, $J = 7.0$ Hz, 1H), 6.71 (d, $J = 8.0$ Hz, 1H), 6.66 (t, $J = 6.8$ Hz, 1H), 6.32 (d, $J = 7.5$ Hz, 3H), 3.93 (s, 6H), 3.86 (s, 3H), 2.82 (s, 3H). ^{13}C NMR (151 MHz, DMSO-d_6) δ 188.54, 168.25, 163.16, 161.31, 150.05, 143.20, 134.56, 133.25, 133.05, 129.05, 128.91, 120.35, 119.72, 115.33, 114.14, 110.78, 105.21, 91.04, 56.06, 55.52, 29.42. IR (ATR) V_{max} cm^{-1}: 3355 (N-H stretching), 1647 (C=O stretching), 1590 (C=C stretching), 1294 (C-O stretching) and 743 (C-H bending). The HRMS (APCI) *m/z* $[M + H]^+$ calculated for $C_{26}H_{27}N_2O_5$ 447.1908; found 447.1908. Purity (HPLC): 100%. R_t: 2.2 min.

(E)-N-(4-(3-(3-methoxyphenyl)acryloyl)phenyl)-2-(methylamino)benzamide (K17)

Grey powder, yield of 51.38% and m. pt. 130.4 °C. ^{1}H NMR (600 MHz, DMSO-d_6) δ 10.40 (s, 1H), 8.19 (d, $J = 6.3$ Hz, 2H), 7.99 (s, 1H), 7.95 (d, $J = 7.8$ Hz, 2H), 7.72 (s, 1H), 7.70 (s, 1H), 7.49 (s, 1H), 7.44 (s, 1H), 7.41–7.31 (m, 3H), 7.03 (s, 1H), 6.71 (d, $J = 7.9$ Hz, 1H), 6.66 (s, 1H), 3.84 (s, 3H), 2.81 (s, 3H). ^{13}C NMR (151 MHz, DMSO-d_6) δ 187.56, 168.32, 159.63, 150.21, 143.84, 143.27, 136.17, 133.13, 132.30, 129.85, 129.59, 129.06, 122.27, 121.54, 119.59, 116.50, 115.09, 114.01, 113.31, 110.71, 55.28, 29.35. IR (ATR) V_{max} cm^{-1}: 3371 (N-H stretching), 1652 (C=O stretching), 1602 (C=C stretching), 1289 (C-O stretching) and 743 (C-H bending). The HRMS (APCI) *m/z* $[M + H]^+$ calculated for $C_{24}H_{23}N_2O_3$ 387.1695; found 387.1695. Purity (HPLC): 98%. R_t: 2.2 min.

(E)-N-(4-(3-(2-bromophenyl)acryloyl)phenyl)-2-(methylamino)benzamide (K18)

Mustard powder, yield of 61.64% and m. pt. 130.7–134.1 °C. ^{1}H NMR (600 MHz, DMSO-d_6) δ 10.43 (s, 1H), 8.22–8.18 (m, 3H), 7.99 (s, 2H), 7.95 (d, $J = 8.7$ Hz, 2H), 7.75 (d, $J = 7.3$ Hz, 1H), 7.73–7.71 (m, 1H), 7.50 (t, $J = 7.3$ Hz, 1H), 7.41–7.39 (m, 1H), 7.38 (d, $J = 7.0$ Hz, 1H), 7.34 (d, $J = 5.2$ Hz, 1H), 6.71 (d, $J = 8.3$ Hz, 1H), 6.66 (t, $J = 7.3$ Hz, 1H), 2.81 (d, $J = 4.9$ Hz, 3H). ^{13}C NMR (151 MHz, DMSO-d_6) δ 187.34, 168.42, 150.27, 144.18, 140.66, 134.10, 133.30, 133.24, 132.07, 129.82, 129.16, 128.74, 128.24, 125.33, 124.93, 119.67, 115.08, 114.07, 110.77, 29.42. IR (ATR) Vmax cm-1: 3359 (N-H stretching), 1650 (C=O stretching), 1590 (C=C stretching), 754 (C-Br stretching) and 736 (C-H bending). The HRMS (APCI) m/z $[M + H]^+$ calculated for $C_{23}H_{20}BrN_2O_2$ 435.0686; found 435.0703. Purity (HPLC): 95%. R_t: 2.2 min.

(E)-N-(4-(3-(2,5-dimethoxyphenyl)acryloyl)phenyl)-2-(methylamino)benzamide (K19)

Brown powder, yield of 50.25% and m. pt. 102.2–102.3 °C. ^{1}H NMR (600 MHz, DMSO-d_6) δ 10.40 (s, 1H), 8.18 (s, 2H), 7.98 (d, $J = 43.7$ Hz, 3H), 7.72 (s, 1H), 7.57 (s, 2H), 7.51–7.28 (m, 2H), 7.05 (s, 2H), 6.70 (s, 1H), 6.67 (s, 1H), 3.85 (s, 3H), 3.81 (s, 3H), 2.81 (s, 3H). ^{13}C NMR (151 MHz, DMSO-d_6) δ 187.66, 168.31, 153.25, 152.64, 150.20, 143.74, 137.56, 133.11, 132.45, 129.52, 129.06, 123.63, 121.99, 119.59, 117.93, 115.11, 114.01, 113.02, 112.56, 110.70, 56.14, 55.68, 29.35. IR (ATR) V_{max} cm^{-1}: 3311 (N-H stretching), 1648 (C=O stretching), 1591 (C=C stretching), 1233 (C-O stretching) and 742 (C-H bending). The HRMS (APCI) m/z $[M + H]^+$ calculated for $C_{25}H_{25}N_2O_4$ 417.1799; found 417.1799. Purity (HPLC): 99%. R_t: 2.2 min.

(E)-2-(methylamino)-N-(4-(3-(thiophen-3-yl)acryloyl)phenyl) benzamide (K20)

Light mustard powder, yield of 51.82% and m. pt. 114.9 °C. ^{1}H NMR (600 MHz, DMSO-d_6) δ 10.40 (s, 1H), 8.15 (d, $J = 8.7$ Hz, 2H), 8.10 (d, $J = 1.7$ Hz, 1H), 7.94 (d,

$J = 8.7$ Hz, 2H), 7.79 (d, $J = 15.4$ Hz, 2H), 7.76 (s, 1H), 7.72 (dd, $J = 11.1$, 4.2 Hz, 1H), 7.67 (dd, $J = 4.7$, 2.9 Hz, 1H), 7.38 (t, $J = 7.2$ Hz, 1H), 7.34 (d, $J = 4.5$ Hz, 1H), 6.71 (d, $J = 8.3$ Hz, 1H), 6.66 (t, $J = 7.2$ Hz, 1H), 2.81 (d, $J = 4.8$ Hz, 3H). ^{13}C NMR (151 MHz, DMSO-d_6) δ 187.80, 168.39, 150.25, 143.86, 138.34, 137.20, 133.19, 132.42, 130.34, 129.52, 129.14, 127.66, 126.19, 121.49, 119.64, 115.16, 114.07, 110.75, 29.42. IR (ATR) V_{max} cm^{-1}: 3339 (N-H stretching), 1650 (C=O stretching), 1592 (C=C stretching), 2813 (S-H stretching) and 743 (C-H bending). The HRMS (APCI) m/z $[M + H]^+$ calculated for $C_{21}H_{19}N_2O_5S$ 363.1162; found 363.1139. Purity (HPLC): 99%. R_t: 2.2 min.

(E)-2-(methylamino)-N-(4-(3-(thiophen-2-yl)acryloyl)phenyl) benzamide (K21)

Mustard powder, yield of 51.82% and m. pt. 146.3 °C. ^{1}H NMR (600 MHz, DMSO-d_6) δ 10.38 (s, 1H), 8.11 (d, $J = 8.0$ Hz, 2H), 7.95–7.91 (m, 3H), 7.89 (s, 1H), 7.78 (d, $J = 4.3$ Hz, 1H), 7.72 (d, $J = 7.7$ Hz, 1H), 7.68 (s, 1H), 7.59 (d, $J = 15.3$ Hz, 1H), 7.38 (t, $J = 7.7$ Hz, 1H), 7.20 (s, 1H), 6.71 (d, $J = 8.3$ Hz, 1H), 6.66 (t, $J = 7.3$ Hz, 1H), 2.82 (s, 3H). ^{13}C NMR (151 MHz, DMSO-d_6) δ 187.01, 168.30, 150.19, 143.76, 139.79, 136.03, 133.11, 132.48, 132.23, 130.12, 129.39, 129.06, 128.61, 120.32, 119.64, 115.10, 114.02, 110.71, 29.36. IR (ATR) V_{max} cm^{-1}: 3322 (N-H stretching), 1645 (C=O stretching), 1593 (C=C stretching), 2360 (S-H stretching) and 735 (C-H bending). The HRMS (APCI) *m/z* $[M + H]^+$ calculated for $C_{21}H_{19}N_2O_2S$ 363.1135; found 363.1135. Purity (HPLC): 98%. R_t: 2.2 min.

(E)-N-(4-(3-(benzo[d][1,3]dioxol-5-yl)acryloyl)phenyl)-2-(methylamino)benzamide (K22)

Light yellow powder, yield of 67.01% and m. pt. 135.1 °C. ^{1}H NMR (600 MHz, DMSO-d_6) δ 10.39 (s, 1H), 8.17 (d, $J = 8.7$ Hz, 2H), 7.93 (d, $J = 8.7$ Hz, 2H), 7.85 (d, $J = 15.5$ Hz, 1H), 7.74–7.70 (m, 1H), 7.69–7.65 (m, 2H), 7.40–7.31 (m, 3H), 7.00 (d, $J = 8.0$ Hz, 1H), 6.70 (d, $J = 8.3$ Hz, 1H), 6.66 (t, $J = 7.4$ Hz, 1H), 6.11 (s, 2H), 2.81 (d, $J = 4.7$ Hz, 3H). ^{13}C NMR (151 MHz, DMSO-d_6) δ 187.38, 168.38, 150.25, 149.47, 148.11, 143.83, 143.37, 133.18, 132.53, 129.54, 129.36, 129.14, 125.82, 119.96, 119.63, 115.18, 114.06, 110.75, 108.54, 106.94, 101.65, 29.42. IR (ATR) V_{max} cm^{-1}: 3420 (N-H stretching), 1656 (C=O stretching), 1588 (C=C stretching), 1217 (C-O stretching) and 746 (C-H bending). The HRMS (APCI) *m/z* $[M + H]^+$ calculated for $C_{24}H_{21}N_2O_4$ 401.1472; found 401.1472. Purity (HPLC): 99%. R_t: 2.2 min.

(E)-2-(methylamino)-N-(4-(3-(2,4,5-trimethoxyphenyl) acryloyl)phenyl)benzamide (K23)

Yellow powder, yield of 60.09% and m. pt. 121.3–123.0 °C. ^{1}H NMR (600 MHz, DMSO-d_6) δ 10.39 (s, 1H), 8.16 (d, $J = 8.7$ Hz, 1H), 8.06 (d, $J = 15.6$ Hz, 1H), 7.96–7.93 (m, 1H), 7.92 (s, 1H), 7.88 (d, $J = 8.7$ Hz, 1H), 7.78 (t, $J = 11.9$ Hz, 1H), 7.71 (t, $J = 7.6$ Hz, 1H), 7.53 (s, 1H), 7.37 (dd, $J = 16.1$, 9.0 Hz, 1H), 7.33 (s, 1H), 6.75 (s, 1H), 6.70 (dd, $J = 8.2$, 3.8 Hz, 1H), 6.66 (t, $J = 7.0$ Hz, 1H), 3.92–3.89 (m, 3H), 3.87 (s, 3H), 3.83 (s, 3H), 2.81 (t, $J = 4.5$ Hz, 3H). ^{13}C NMR (151 MHz, DMSO) δ 186.83, 168.37, 154.19, 152.78, 150.23, 143.11, 137.87, 133.17, 132.85, 129.42, 129.19, 129.13, 119.61, 119.53, 118.64, 115.22, 114.08, 110.97, 110.74, 97.58, 56.44, 55.84, 29.42, 26.46. IR (ATR) V_{max} cm^{-1}: 3337 (N-H stretching), 1651 (C=O stretching), 1591 (C=C stretching) 1266 (C-O stretching) and 743 (C-H bending). The HRMS (APCI) m/z $[M + H]^+$ calculated for $C_{26}H_{27}N_2O_5$ 447.1898; found 447.1898. Purity (HPLC): 95%. R_t: 2.2 min.

(E)-N-(4-(3-(2-methoxyphenyl)acryloyl)phenyl)-2-(methylamino)benzamide (K25)

Light yellow powder, yield of 69.43% and m. pt. 143.8 °C. ^{1}H NMR (600 MHz, DMSO-d_6) δ 10.40 (s, 1H), 8.15 (d, $J = 8.7$ Hz, 2H), 8.05 (d, $J = 15.7$ Hz, 1H), 7.99 (d, $J = 7.1$ Hz, 1H), 7.95–7.92 (m, 2H), 7.90 (s, 1H), 7.72 (d, $J = 7.1$ Hz, 1H), 7.45 (t, $J = 7.2$ Hz, 1H), 7.38 (t, $J = 7.5$ Hz, 1H), 7.34 (d, $J = 4.6$ Hz, 1H), 7.12 (d, $J = 8.3$ Hz, 1H), 7.04 (t, $J = 7.5$ Hz, 1H), 6.70 (d, $J = 8.4$ Hz, 1H), 6.66 (t, $J = 7.3$ Hz, 1H), 3.90 (s, 3H), 2.81 (d, $J = 4.9$ Hz, 3H). ^{13}C NMR (151 MHz, DMSO-d_6) δ 187.73, 168.38, 158.21, 150.25, 143.82, 137.85, 133.20, 132.50, 132.19, 129.54, 129.14, 128.39, 123.07, 121.79, 120.70, 119.68, 115.15, 114.07, 111.80, 110.76, 55.74, 29.42. IR (ATR) V_{max} cm^{-1}: 3322 (N-H stretching), 1647 (C=O stretching), 1590 (C=C stretching), 1126 (C-O stretching) and 738 (C-H bending). The HRMS (APCI) *m/z* $[M + H]^+$ calculated for $C_{24}H_{23}N_2O_3$ 387.1683; found 387.1683. Purity (HPLC): 98%. R_t: 2.2 min.

In vitro anti-parasitic assay

Anti-parasitic assays were performed as described elsewhere [41, 42]. Briefly, to evaluate anti-*Leishmania* activity, *L. infantum* [MHOM/ MA (BE)/67] was used with primary peritoneal mouse macrophages as host cells. 3×10^4 macrophages were infected with 4.5×10^5 parasites per well. Compound dilutions were added after 2 h of infection. After 5 days of incubation, parasite burdens (mean number of amastigotes/macrophage) were assessed microscopically after staining with a 10% Giemsa solution.

For *T. cruzi*, the Tulahuen CL2, β-galactosidase strain (nifurtimox-sensitive) was used and maintained on MRC-5_{SV2} (human lung fibroblast). 4×10^3 cells were infected with 4×10^4 parasites per well. Parasite burdens were assessed after adding the substrate CPRG (chlorophenol red β-d- galactopyranoside). The change in color was measured spectrophotometrically at 540 nm after 4 h incubation at 37 °C. Drug susceptibility tests for *T. brucei* were performed using a resazurin assay. Susceptibility assays were performed with *T. brucei* Squib 42749 or *T. b. rhodesiense* STIB-90050. *T. brucei* Squib 427 was seeded at 1.5×10^4 parasites/well and *T. b. rhodesiense* at 4×10^3 parasites per well, followed by the addition of resazurin after 24 h (*T. brucei*) or 6 h (*T. b. rhodesiense*). After the addition of resazurin, plates were incubated for another 24 h followed by fluorescence detection (λ_{ex} 550 nm, λ_{em} 590 nm).

In all assays, parasite growth was compared to untreated-infected controls (100% growth) and noninfected controls (0% growth). Results were expressed as % parasite reduction at the different drug concentrations and used to calculate IC_{50} values from the dose–response curves.

In vitro cytotoxicity

MRC-5_{SV2} cell cytotoxicity was evaluated as described elsewhere [41]. Briefly, 1.5×10^5 cells/ mL cells were cultured with compound dilutions at 37 °C and with 5% CO_2. Cell growth was compared to untreated-control wells (100% cell growth) and medium-control wells (0% cell growth). After 3 days of incubation, cell viability was assessed fluorimetrically after the addition of 50 µL resazurin per well. After 4 h at 37 °C, fluorescence was measured. The results were expressed as a % reduction in cell growth/ viability compared to control wells and an IC_{50} value was determined.

Conclusion

Parasitic diseases remain a critical global health issue. Aside from their potential fatality, several presently available medications have inherent drawbacks, such as toxicity, questionable efficacy, extended treatment durations, and the emergence of resistance. Twenty-one new chalcone derivatives were synthesized, characterized utilizing variety of spectrometry/spectroscopy techniques such as ^1H and ^{13}C NMR & HRMS, and evaluated for their in vitro antiparasitic activities. Two compounds, **K4** and **K9**, stand out as particularly promising, demonstrating significant activity in the low micromolar range against both *T. b. brucei* and *T. b. rhodesiense*. These compounds demonstrated no inhibitory impact on human cells (MRC-5). Specifically, **K4** exhibited a selectivity index (SI) of 160 for *T. b. brucei* and 52 for *T. b. rhodesiense*, respectively. These compounds deserve further preclinical exploration of their therapeutic activity against African trypanosomes.

Data availability

The supporting data for the conclusions of this study can be found in the supplementary material provided with this article.

Supplementary information The online version contains supplementary material available at https://doi.org/10.1007/s00044-024-03235-x.

Acknowledgements LMPH is a partner of the Excellence Centre 'Infla-Med' (www.uantwerpen.be/infla-med) and participates in COST Action CA21111.

Author contributions KJS synthesis the compounds, wrote first draft of the manuscript. RMB supervised the work. KI and DM performed bioassay. GC supervised and validated the assays. LJL designed the project. All authors revised the manuscript.

Funding Open access funding provided by North-West University. This research was funded by the South African National Research Foundation (NRF) and the North-West University.

Compliance with ethical standards

Conflict of interest The authors declare no competing interests.

References

1. Kennedy PGE, Rodgers J. Clinical and neuropathogeneticaspects of human african trypanosomiasis. Front Immunol. 2019;10:39. https://doi.org/10.3389/fimmu.2019.00039.
2. Simarro PP, Cecchi G, Paone M, Franco JR, Diarra A, Ruiz JA, et al. The Atlas of human African trypanosomiasis: a contribution to global mapping of neglected tropical diseases. Int J Health Geographics. 2010;9:1–18. https://doi.org/10.1186/1476-072X-9-57.
3. Venturelli A, Tagliazucchi L, Lima C, Venuti F, Malpezzi G, Magoulas GE, et al. Current treatments to control african trypanosomiasis and one health perspective. Microorganisms. 2022;10:1298. https://doi.org/10.3390/microorganisms10071298.

4. Inocencio da Luz R, Tablado Alonso S, Büscher P, Verlé P, De Weggheleire A, Mumba Ngoyi D, et al. Two-year follow-up of Trypanosoma brucei gambiense serology after successful treatment of human african trypanosomiasis: Results of four different sero-diagnostic tests. Diagnostics. 2022;12:246. https://doi.org/10.3390/diagnostics12020246.
5. Idro R, Ogwang R, Barragan A, Raimondo JV, Masocha W. Neuroimmunology of common parasitic infections in Africa. Front Immunol 2022;13:791488.
6. De Koning HP. The drugs of sleeping sickness: their mechanisms of action and resistance, and a brief history. Tropical Med Infect Dis. 2020;5:14. https://doi.org/10.3390/tropicalmed5010014.
7. Kansiime F, Adibaku S, Wamboga C, Idi F, Kato CD, Yamuah L, et al. A multicentre, randomised, non-inferiority clinical trial comparing a nifurtimox-eflornithine combination to standard eflornithine monotherapy for late stage Trypanosoma brucei gambiense human African trypanosomiasis in Uganda. Parasites Vectors. 2018;11:1–11. https://doi.org/10.1186/s13071-018-2634-x.
8. Lindner AK, Lejon V, Chappuis F, Seixas J, Kazumba L, Barrett MP, et al. New WHO guidelines for treatment of gambiense human African trypanosomiasis including fexinidazole: substantial changes for clinical practice. Lancet Infect Dis. 2020;20:e38–e46. https://doi.org/10.1016/S1473-3099(19)30612-7.
9. Helleberg BB, Gudmundsson KSS, Kurtzhals JAL, Helleberg M. Second stage human African Trypanosomiasis with Trypanosoma brucei rhodesiense treated with fexinidazole. Lancet Infect Dis. 2023;23:e505. https://doi.org/10.1016/S1473-3099(23)00358-4.
10. Pelosse P, Kribs-Zaleta CM. The role of the ratio of vector and host densities in the evolution of transmission modes in vector-borne diseases. The example of sylvatic Trypanosoma cruzi. J Theor Biol. 2012;312:133–42.
11. Ayres J, Marcus R, Standley CJ. The Importance of Screening for Chagas Disease Against the Backdrop of Changing Epidemiology in the USA. Curr Tropical Med Rep. 2022;9:185–93. https://doi.org/10.1007/s40475-022-00264-7.
12. Fiatsonu E, Busselman RE, Ndeffo-Mbah ML. A Scoping Review of Mathematical Models Used to Investigate the Role of Dogs in Chagas Disease Transmission. Animals. 2023;13:555. https://doi.org/10.3390/ani13040555.
13. Forsyth CJ, Hernandez S, Flores CA, Roman MF, Nieto JM, Marquez G, et al. You Don't Have a Normal Life": Coping with Chagas Disease in Los Angeles, California. Med Anthropol. 2021;40:525–40. https://doi.org/10.1080/01459740.2021.1894559.
14. Ocaña-Mayorga S, Bustillos JJ, Villacís AG, Pinto CM, Brenière SF, Grijalva MJ. Triatomine feeding profiles and Trypanosoma cruzi infection, implications in domestic and sylvatic transmission cycles in Ecuador. Pathogens. 2021;10:42. https://doi.org/10.3390/pathogens10010042.
15. Hyson P, Barahona LV, Pedraza-Arévalo LC, Schultz J, Mestroni L, da Consolação Moreira M, et al. Experiences with diagnosis and treatment of Chagas disease at a United States teaching hospital—clinical features of patients with positive screening serologic testing. Tropical Med Infect Dis. 2021;6:93. https://doi.org/10.3390/tropicalmed6020093.
16. Lidani KCF, Andrade FA, Bavia L, Damasceno FS, Beltrame MH, Messias-Reason IJ, et al. Chagas disease: from discovery to a worldwide health problem. Front Public Health. 2019;7:166. https://doi.org/10.3389/fpubh.2019.00166.
17. Chatelain E. Chagas disease research and development: Is there light at the end of the tunnel? Comput Struct Biotechnol J. 2017;15:98–103. https://doi.org/10.1016/j.csbj.2016.12.002.
18. Moncayo Á, Silveira AC. Current epidemiological trends of Chagas disease in Latin America and future challenges: Epidemiology, surveillance, and health policies. Am Trypanosomiasis Chagas Dis. 2017:59–88 https://doi.org/10.1590/s0074-02762009000900005.
19. Tarleton RL, Reithinger R, Urbina JA, Kitron U, Gürtler RE. The challenges of Chagas disease—grim outlook or glimmer of hope? PLoS Med. 2007;4:e332. https://doi.org/10.1371/journal.pmed.0040332.
20. Lee BY, Bacon KM, Bottazzi ME, Hotez PJ. Global economic burden of Chagas disease: a computational simulation model. Lancet Infect Dis. 2013;13:342–8. https://doi.org/10.1016/S1473-3099(13)70002-1.
21. Bonney KM. Chagas disease in the 21st century: a public health success or an emerging threat? Parasite. 2014;21:1–10. https://doi.org/10.1051/parasite/2014012.
22. Liu Q, Zhou X-N. Preventing the transmission of American trypanosomiasis and its spread into non-endemic countries. Infect Dis Poverty. 2015;4:1–11. https://doi.org/10.1186/s40249-015-0092-7.
23. Lascano F, García Bournissen F, Altcheh J. Review of pharmacological options for the treatment of Chagas disease. Br J Clin Pharmacol. 2022;88:383–402. https://doi.org/10.1111/bcp.14700.
24. Setshedi KJ, Beteck RM, Jesumoroti OJ, Ilbeigi K, Mabille D, Caljon G, et al. 2-Aroyl quinazolinone: Synthesis and in vitro antiparasitic activity. Chem Biol Drug Des. 2023;102:763–72. https://doi.org/10.1111/cbdd.14284.
25. Jackson Y, Wyssa B, Chappuis F. Tolerance to nifurtimox and benznidazole in adult patients with chronic Chagas' disease. J Antimicrobial Chemother. 2020;75:690–6. https://doi.org/10.1093/jac/dkz473.
26. Ciapponi A, Barreira F, Perelli L, Bardach A, Gascon J, Molina I, et al. Fixed vs adjusted-dose benznidazole for adults with chronic Chagas disease without cardiomyopathy: a systematic review and meta-analysis. PLoS Neglected Tropical Dis. 2020;14:e0008529. https://doi.org/10.1371/journal.pntd.0008529.
27. Crespillo-Andújar C, Comeche B, Hamer DH, Arevalo-Rodriguez I, Alvarez-Díaz N, Zamora J, et al. Use of benznidazole to treat chronic Chagas disease: An updated systematic review with a meta-analysis. PLOS Neglected Tropical Dis. 2022;16:e0010386. https://doi.org/10.1371/journal.pntd.0010386.
28. Machado CAL, da Paixão Sevá A, Dantas-Torres F, Horta MC. Spatial analysis and epidemiological profile of visceral leishmaniasis, northeastern Brazil: A cross-sectional study. Acta Tropica. 2020;208:105520. https://doi.org/10.1016/j.actatropica.2020.105520.
29. Gültekin M, Karakuş M, Seray T, Voyvoda H. First clinical case of leishmaniosis due to Leishmania infantum in a domestic cat from Turkey. Anim Health Prod Hyg. 2020;9:734–7.
30. Ruiz-Postigo J, Jain S, Madjou S, Maia-Elkhoury A, Valadas S, Warusavithana S, et al. Global leishmaniasis surveillance: 2021, assessing the impact of the COVID-19 pandemic. Weekly Epidemiological Record. 2022:97;575–90.
31. WHO. WHO guideline for the treatment of visceral leishmaniasis in HIV co-infected patients in East Africa and South-East Asia. Geneva: World Health Organization; 2022.
32. Scarpini S, Dondi A, Totaro C, Biagi C, Melchionda F, Zama D, et al. Visceral leishmaniasis: epidemiology, diagnosis, and treatment regimens in different geographical areas with a focus on pediatrics. Microorganisms. 2022;10:1887. https://doi.org/10.3390/microorganisms10101887.
33. Ghosh P, Roy P, Chaudhuri SJ, Das NK. Epidemiology of post-Kala-Azar dermal leishmaniasis. Indian J Dermatol. 2021;66:12. https://doi.org/10.4103/ijd.IJD_651_20.
34. Pokharel P, Ghimire R, Lamichhane P. Efficacy and safety of paromomycin for visceral leishmaniasis: A systematic review. J Trop Med. 2021;2021 https://doi.org/10.1155/2021/8629039.

35. Ouyang Y, Li J, Chen X, Fu X, Sun S, Wu Q. Chalcone derivatives: Role in anticancer therapy. Biomolecules. 2021;11:894. https://doi.org/10.3390/biom11060894.
36. Mezgebe K, Melaku Y, Mulugeta E. Synthesis and Pharmacological Activities of Chalcone and Its Derivatives Bearing N-Heterocyclic Scaffolds: A Review. ACS Omega. 2023;8:19194–211. https://doi.org/10.1021/acsomega.3c01035.
37. Elkanzi NA, Hrichi H, Alolayan RA, Derafa W, Zahou FM, Bakr RB. Synthesis of chalcones derivatives and their biological activities: a review. ACS Omega. 2022;7:27769–86. https://doi.org/10.1021/acsomega.2c01779.
38. Goyal K, Kaur R, Goyal A, Awasthi R. Chalcones: A review on synthesis and pharmacological activities. J Appl Pharm Sci. 2021;11:001–14.
39. Lahsasni SA, Korbi A, Hamad F, Aljaber NA-A. Synthesis, characterization and evaluation of antioxidant activities of some novel chalcones analogues. Chem Cent J. 2014;8:1–10. https://doi.org/10.1186/1752-153X-8-32.
40. Beteck RM, Legoabe LJ, Isaacs M, Khanye SD, Laming D, Hoppe HC. Anti-trypanosomal and antimalarial properties of tetralone derivatives and structurally related benzocycloalkanones. Medicina. 2019;55:206.
41. Bouton J, d'Almeida AF, Maes L, Caljon G, Van Calenbergh S, Hulpia F. Synthesis and evaluation of 3′-fluorinated 7-deazapurine nucleosides as antikinetoplastid agents. Eur J Med Chem. 2021;216:113290. https://doi.org/10.1016/j.ejmech.2021.113290.
42. Hulpia F, Mabille D, Campagnaro GD, Schumann G, Maes L, Roditi I, et al. Combining tubercidin and cordycepin scaffolds results in highly active candidates to treat late-stage sleeping sickness. Nat Commun. 2019;10:5564. https://doi.org/10.1038/s41467-019-13522-6.
43. Boeck P, Falcão CAB, Leal PC, Yunes RA, Cechinel FV, Torres-Santos EC, et al. Synthesis of chalcone analogues with increased antileishmanial activity. Bioorg Med Chem. 2006;14:1538–45. https://doi.org/10.1016/j.bmc.2005.10.005.
44. Ortalli M, Ilari A, Colotti G, De Ionna I, Battista T, Bisi A, et al. Identification of chalcone-based antileishmanial agents targeting trypanothione reductase. Eur J Med Chem. 2018;152:527–41. https://doi.org/10.1016/j.ejmech.2018.04.057.
45. Escrivani DO, Charlton RL, Caruso MB, Burle-Caldas GA, Borsodi MPG, Zingali RB, et al. Chalcones identify cTXNPx as a potential antileishmanial drug target. PLoS Negl Trop Dis. 2021;15:e0009951. https://doi.org/10.1371/journal.pntd.0009951.